Study and evaluation of salt fog phenomenon on the excavated pottery sherds surface

Elshaimaa Abd Elrahim and Hamdy Mohamed Mohamed*

Conservation Department, Faculty of Archaeology, Cairo University, 12613 Giza, Egypt.

*Corresponding author: Hamdy Mohamed Mohamed (hamdy.mohamed@cu.edu.eg)

Unedited version published online on 18/10/2023

Abstract

A strange phenomenon attracted our team to the study of the presence of saline fog on pottery surfaces. Besides, the crystallization of salts during drying leads to pottery damage. A significant step is examining the salts to recognize their kinds and identify the chemical composition of the sherds. For this purpose, a visual assessment, a digital microscope, and a scanning electron microscope with EDX (SEM-EDX) were used to detect surface deterioration. In addition, X-ray diffraction (XRD) and Fourier transform infrared spectroscopy (FTIR) analysis were carried out to identify the chemical composition of potsherds and salts. The microscopic investigation revealed a dense distribution of salt on the potsherd surface. Besides, the SEM micrograph shows clear cubic salt crystals of sodium chloride, especially after drying. Moreover, SEM-EDX analysis revealed high chloride salt concentrations, in addition to silica and aluminum oxide, which are the primary ingredients in pottery making. According to XRD analysis, the pottery samples primarily contain diopside, hematite, magnetite, albite, and muscovite, which are the primary components in manufacturing. Furthermore, halite appears in large proportions due to the influence of the burial soil. Besides, the pottery samples' quartz, clay minerals, hematite, and calcite contents were confirmed by FTIR. The results generally support the widely held belief that sodium chloride significantly influences archaeological pottery.

Keywords: Pottery, Salt efflorescence, deterioration, SEM-EDX, XRD, FTIR.

Introduction

Archaeological pottery is historically significant because its information helps historians understand ancient cultures[1]. Furthermore, pottery can be used to discover more information about the location; the people interred there, and the significant religious practices of their descendants who came to the site in later centuries[2]. Several potsherds from the New Kingdom period in Egypt were discovered during the 2020 season at the Saqqara excavation site of Cairo University's Faculty of Archeology. For thousands of years, Saqqara has held great historical and cultural significance. Pottery is the most frequent artifact discovered during excavation[3]. The New Kingdom was a time of widespread prosperity, as reflected in the pottery industry. Moreover, the pottery of this period is well made[4].

Water has an indirect effect by transporting soluble salts, one of the primary causes of artifact deterioration[5]. Because water penetrates the pores, the pottery deteriorates due to salts, particularly soluble salt[6]. The most common cause of the salt attack is increased moisture in the soil[7]. Therefore, water penetration into archaeological objects is considered the primary cause of degradation, especially in porous materials[8]. When salt is dissolved in water, it can be transferred through a porous substance. Salt is carried to the evaporation front during surface drying, crystallizing and accrues[9]. When it comes to the crystallization of soluble salts, temperature plays a significant role. Salts crystallize more quickly at higher temperatures, whether inside the body or on an external surface[10].

Salt crystallization in porous materials is a common cause of archaeological object damage[9]. Porosity has a vital role in the deterioration processes of archaeological pottery because

Unedited version published online on 18/10/2023

the pore network permits the penetration of water, which is accountable for the various chemical and physical damage processes influencing the pottery body[11]. Salt dramatically affects the durability of archaeological pottery. Therefore, their study is critical to comprehending the crystallization process inside the pottery body. This will help discover a strategy to prevent or limit their harm to porous materials[12]. Soluble salts severely decrease the porous materials' durability.

Consequently, preventing salt crystallization requires understanding the mechanisms that cause it[13]. The penetration of salt solutions into the body's interior pores generates fissures, while the crystallization of these salts on the exterior surface causes the surface decorations to be distorted[14]. The most popular theory proposes that when water evaporates or the temperature rises, a saline solution is spread inside body pores, where salt efflorescence starts. The permeability and pore size of the pottery, as well as the ambient temperature and relative humidity, impact the evaporation rate[15].

The types and salt concentrations found on pottery surfaces vary widely, depending on the kind of pottery and the location in which it is found[16]. However, salt fog activities also include the crystallization and deposit of salt fog on the surface of these objects. Potsherd pores become voids because of salt expansion after salt solution seeps into the pores[17]. The pore structure and saturation level influence the crystallization degree in porous materials. The pressure of crystallization is known to be lower in larger pores. Furthermore, high saturation levels result in high crystallization pressures. Furthermore, salt crystallization primarily occurs on porous pottery's surface (efflorescence)[13]. Several factors influence the high saturation degree, including the initial solution concentration, relative humidity, temperature, substrate roughness, and surface area[18].

This study concerns the pottery sherds being affected by a salt solution that appears on its surface within hours of its extraction and then dried and crystallized in Saqqara excavations. To

Unedited version published online on 18/10/2023

understand why salt crystallization interacts with dissolving and how quickly evaporated water causes microcrystallization, it was essential to explain how salt crystallizes and dissolves. Though sodium chloride has been extensively studied for various applications, the crystallization mechanism is still not fully understood. Studies on this phenomenon are rare, and this interaction's physical and mechanical deterioration is poorly known. Excavated surroundings negatively affect archaeological findings through physical or chemical processes based on material properties. The research aims to study this strange phenomenon, which appears on the excavated pottery surface and damages it, in addition to determining the influence of salts' precipitation on the pottery's porous structure. Understanding how salt crystallization affects the deterioration of porous pottery is critical for cultural heritage preservation.

Unedited Version published online on 18/10/2023

Materials and Methods

Materials

Two potsherds were taken from the Faculty of Archeology, Cairo University's excavations at Saqqara, to study the damage mechanism and define the role of the salts in the deterioration. The excavated sherds varied in size from small, and large. The potsherds were coded to facilitate the discussion, as shown in Table 1.

Methods of Analysis

Visual Assessment

Using a camera of the SONY brand, the sample surfaces were examined. Specifications for cameras are (16 megapixels CMOS beam, 8x optical zoom, up to clear 16x picture zoom, 25mm wide-angle lens (35mm format), and full HD movie (1920 * 1080)).

Digital Microscope

Sensor CMOS HD with a digital zoom of 5x, high-speed DSP (drive free offered), 24-bit DSP, USB 3.0 and USB 2.0 compatibility, super-resolution 640*480 to 1600*1200.

Scanning Electron Microscope with Elemental Analysis Unit (SEM-EDX)

This study connected an EDX unit to SEM Model Quanta 250 FEG (Field Emission Gun) (Energy Dispersive X-ray Analyzes). Specifications: resolutions for Gun.1n), FEI Company, Netherlands; 30 KV accelerating voltage; magnification 14x to 1000000.

Analysis of X-ray diffraction (XRD)

Cu-radiation (λ=1.542Å) was applied with a secondary monochromator on a PANanalytical X-Ray Diffraction equipment model XPert PRO at 45 KV, 35 MA, and a scanning speed of 0.04 o/sec. The relative intensities (I/I^o), corresponding spacings (d, Å), and diffraction peaks were measured between $2\theta = 2^o$ and 60^o. Diffraction charts and relative intensities are collected and compared with ICDD data

Fourier Transform Infrared Spectroscopy (FTIR)

A Nicolet 380 FT-IR Spectrometer (Madison, WI, USA) was used to analyze the pottery samples using the solid-sample potassium bromide technique with a resolution of 4 cm^{-1} ranging from 400 to 4000 cm^{-1}. The computer program Spectrum One was used to perform additional processing on the obtained FTIR spectra (ver. 5.0.1)

Results and discussion

Visual Assessment

The chosen excavated potsherds were studied by the naked eye, in addition to using magnifying lenses with (10×-20×) to determine the surface features, the strange transparent drops, a dried crystal of saline solution on the excavated pottery sherds, in addition the appearance of its fabric. Other aspects of deterioration may be discovered by observation and visual assessment. For

Unedited version published 3/10/2023

example, morphologies of NaCl salts can be identified on the surface of the potsherds[17]. The type of material's surface and the solution saturation level both impact salts' crystallization behavior. On the surface of the potsherds, salt crusts, single, well-formed crystals, and bristly efflorescence were found. In the case of bristly efflorescence, crystals form inside the pores and grow upwards to the surface. The crystal stresses the surrounding material during this process, causing spalling and material loss[7].

Due to the quick evaporation of salt-bearing water, the salt crystallizes at a high pace on the surface of the potsherds[9]. Salt decay is generally considered a temperature/humidity-dependent weathering process caused by salt crystals on the porous material's surface. These crystals are typically very visible[20]. The precipitation of solid particles from supersaturated liquid solutions is a key step in the crystallization process. The main catalyst for crystallization from solutions is the difference in chemical potential between the solution and the solid phase[18]. In our case, there were unclear water drops that had formed on the surface of the potsherds. The drops remain on the surface of the excavated pottery for three to four hours after coming out of the excavations into the exposure environment, then gradually drying out and disappearing, leaving behind small distorted spots or solid protrusions on the surfaces and in the pores (Figure 1).

Digital Microscope

One of the most important tools available to conservators is the digital microscope, whose images help assess the state of an object's deterioration[21]. Through the digital microscope examination, Figure 1a shows the presence of salt on the pottery surface in the form of cohesive crusts overlapping with the pottery body. Besides, A clear dried salt crystal layer covers the sherds' surfaces, penetrating inside and evolving the pores. In addition, the salt efflorescence on the entire degraded surface is rough. At the same time, Figure 1b shows salt crystals in the form of surface

Unedited version published online on 18/10/2023

conglomerates spaced from each other with a relatively large thickness. The salt crystal is obtained when the supersaturation indicating the beginning of crystallisation is reached within the sherds[22].

On the other hand, Figure 1c, d shows a dense spread of salt on the potsherd's surface and an overlap between the layers of salt, dust, and sand scattered on the surface. Repeated salt crystallization and dissolution cycles in the pores caused the pottery to crack and crumble. In the potsherds, efflorescence caused by salt deposits has been observed, resulting in detrimental degradation such as exfoliation and fragmentation[7]. If the rate of evaporation is greater than the rate of solution supply, crystallization forms on the surface of the pottery, resulting in salt efflorescence. This explains why salt crystals are on the surface of the pottery's exterior[15]. Salt crystallization inside the pores of pottery can produce enough stress to create cracks in the potsherd's body[23].

Scanning Electron Microscope with Elemental Analysis Unit (SEM-EDX)

The Examination with a Scanning Electron Microscope (SEM)

SEM is considered one of the most utilized techniques for studying the morphology of pottery[23]. SEM data shows halite precipitates on the pottery surface with an equal distribution in a sample (P1). According to electronic microscopy, salts form at or close to the surface because the dense crystalline structure inside the pottery prevents water and vapor transport[19]. If the evaporation rate is higher than the supply rate of the solution, salts are deposited inside the body's pores. Still, in this case, heavy crystallization occurred on the pottery sherd's outer surface due to the rapid water evaporation rate due to the high temperature of the surrounding medium[15]. Due to salt in-filling pores, porosity decreases nearby the surface. Granular disaggregation and salt crystallization have been noticed at a depth of around 1 cm. The size of the interior pores determines the saline

Unedited version published online on 18/10/2023

solution's capacity to permeate the potsherds. The greater the pore size, the more the saline solution penetrates. On the other hand, the smaller the pore size, the less penetration of the solution into the interior[19] (Figure 3).

In contrast, SEM images of pottery shards in the sample (P2) reveal clear cubic salt crystals of sodium chloride, especially after drying, as observed on sample surfaces due to RH evaporation and temperature rise[18]. The kind of salt crystal depends on various factors, including evaporation average and substrate properties. Cubic crystals will grow if the evaporation rate is low. Any remaining solution may then undergo a creeping mechanism and crystallize as crystals resembling efflorescence. Crystallization from solution can be divided into two steps. Forming new crystals is the first step; their growth is the second, and the solution must be completely saturated[24]. At the end of the drying cycle, the hydrated crystals miss their water and transform into an anhydrous shape with a different white color. This gives a clear view of the film spreading around the droplet at the finale of the evaporation process. It was observed that sodium chloride crystals form more frequently when interacting with a nonpolar area (air or hydrophobic solid)[25]. When the body's pores absorb salt solutions, they cause fissures to form, and when they crystallize outside the body, they distort surface decorations. Rapid evaporation causes the growth of cubic-shaped salt crystals on the surface of the potsherds[14] (Figure 4).

The strange phenomenon acted in the presence of sodium chloride saline fog on excavated pottery sherd surfaces, followed by the crystallization of salts during drying. Water - in the form of RH- consists of molecules. The molecules in vapor form are dynamic, moving rapidly while spaced widely apart. The molecules get slower, less energetic, and closer together as the vapor comes into contact with decreasing air temperatures. The vapor, which contains ion salts, transforms into liquid drops when its energy level becomes low enough and stays in this state for over three or four hours. Then with the rise of temperature

Unedited version published online on 18/10/2023

degrees, the salty drops turned to small and weak crystal salts named efflorescence on the sherd surfaces; they appear in different degrees of intensity[26]. Condensation begins to appear on the pottery's surface when the pottery pores are saturated with much steam to the point where it can no longer be tolerated. Because water molecules are too small to adhere to one another on their own, they latch onto something else, so water needs a surface or nucleation point to condense on[27].

It is clear that the amount of salt crystallization is proportional to its concentration inside the pottery body and that there is a direct and linear relationship between the salinity of the solution, its conductivity, and the degree of crystallization[26]. From the following equations, the conditions for the growth of salt crystals under variable humidity and temperature conditions correspond to the observed elevation rates in the atmosphere.

Published online on 18/10/2023

The well-known rate equations are:

$\frac{dq}{dt}$= time rate of mass transport of water vapor to the droplet = $4\pi D(R')^2[\frac{dp}{dR'}]$ (1)

$\frac{dQ1}{dt}$= time rate of heat transport away from the droplet = $4\pi k(R')^2[\frac{dT}{dR'}]$ (2)

$\frac{dQ2}{dt}$= time rate of heat storage in the droplet = $mc_p\frac{dr}{dt}\frac{dT}{dt}$ (3)

The typical equations for the temperature and vapor-density gradients between r, the droplet radius, and a point infinitely far from r are obtained by integrating (1) and (2) over space. Additionally, it is assumed that the accommodation coefficient is unity and that all of the vapor that diffuses to the droplet condenses on it. Another presumption is that heat storage does not impact droplet growth, allowing for the approximation of dT/dr in (3)[28]. A common occurrence is capillary condensation (CC), which is the production from the vapor of a stable phase when the saturation pressure is below. It might happen between particle surfaces or inside porous materials[29].

The Analysis with Scanning Electron Microscope with EDX

The EDX results from the samples recorded in Table 2 and Figure 5 revealed that the samples contains a great ratio of chloride salts, reaching 53.42% in the sample (P1) and 32.8% in the sample (P2). In addition, sulfate salts are a minor proportion in the sample (P1) of 0.29%. These findings showed the presence of chloride and sulfate salts because of the potsherds' burial in a salty environment, resulting in several physiochemical damages aspects[30]. Furthermore, the aluminum and silica oxide ratios in the clay used to make the potsherds differ between samples. Besides, the calcium oxide found in the samples represents one of the clay additives used to make the potsherds. Based on the pottery's calcium oxide content, noncalcareous and calcareous clays can be distinguished from one another[31].

Moreover, the presence of calcium oxide helps to improve its physical properties, which results in a high-quality product. CaO, SiO_2, and Al_2O_3 react at temperatures above 800 ^oC to create calcium silicates, such as diopside, which reveals a high firing temperature for pottery sherds[32]. The presence of hematite in the samples suggests that the potsherds were made in an oxidizing environment based on the availability of iron oxides[33]. The clay materials contain a rising ratio of SiO_2 and a moderate amount of Al_2O_3, CaO, and MgO. Additionally, a high SiO_2 ratio suggests that quartz minerals predominate over clay minerals, while a low K_2O ratio indicates a low illite content[34].

Analysis of X-ray diffraction (XRD)

X-ray diffraction is the most commonly used method for analyzing the crystalline structural characteristics of archaeological pottery[35]. X-ray diffraction can determine the type of clay used, the industry, the firing impact, and the influence of the burial environment[36]. The samples' XRD

Unedited version published online on 18/10/2023

results are displayed in Table 3 and Figure 6. XRD analysis indicated that the potsherd (P1) contained quartz, halite, diopside, hematite, and magnetite. Quartz is one of the most common minerals in potsherds. The presence of quartz is also a main component in the pottery matrix[37]. Halite is present due to the strong effects of salt solution, crystals in the soil, and fast evaporation of water after excavation. Compared to materials with large pores, porous materials' crystallization compression will be higher, and their interiors will primarily experience mineral precipitation (forming subflorescences). These two facts increase the likelihood that porous materials will deteriorate, lowering their resistance to crystallization[13].

Diopside indicates a high firing temperature, as this compound is present at a temperature ranging from 850°C to 900°C. Furthermore, this indicates that the firing atmosphere is oxidizing. Additionally, hematite is a mineral element used as a colorant in the matrix of various pottery products and in the paint colors used to decorate the pottery's surface, giving the material a reddish hue[38]. Furthermore, the XRD pattern shows that hematite makes up most of the reddish-brown pigment. Furthermore, hematite formation starts at around 800°C. In addition, that means the firing atmosphere is oxidizing[34]. Magnetite is an iron oxide found in abundance in the body's core[3]. Besides, the XRD form displays that the sample (P2) contains quartz, albite, halite, muscovite and diopside. The results show that these sherds have a medium proportion of silica as an additive material considered a part of the sherd's mineral composition[39].

Albite and muscovite are considered the main clay components used in pottery making. Excess salt (NaCl) has been linked to several aspects of deterioration, as the local solution can migrate from the burial soil into the body of the pottery sherd. The rapid water evaporation can result in salt crystallizing on the outer surface, which distorts the optical properties and hides the archaeological pottery's features[33]. Besides, most samples exhibit a red color representing the outer

Unedited version published online on 18/10/2023

slip layer due to the presence of iron minerals[40]. Additionally, iron oxide ratios (Magnetite-Fe_3O_4 and Hematite-Fe_2O_3) in the samples reflect the atmospheric surroundings of fire during industrial. The firing process was likely conducted in a reducing atmosphere if the sample contained magnetite. If the sample contains much hematite, the process was likely conducted in an oxidizing atmosphere[34].

Fourier Transform Infrared Spectroscopy (FTIR)

FTIR analysis was utilized to differentiate between various kinds of clay minerals. Additionally, the FTIR method enables the quick identification of various clay minerals and permits the observation of structural changes brought about by chemical changes in clay minerals[41]. The FTIR analyses conducted on the two samples revealed similarities in the chemical composition of the raw pottery clay, as shown in Table 4 and Figure 7. The range of 4000-3000 cm^{-1} is attributed to water. The absorbed water from the samples was also detected through obvious peaks from 3756, and 3436 cm^{-1} in sample P1 and 3435.56 cm^{-1} in sample P2. This may result from the relative humidity of saline solutions absorbed by halite or the unfired clay found in pottery cores[42]. Besides, these sorbents' IR spectra reveal an absorption band of clay at about 3435 cm^{-1} that corresponds to H_2O vibrations, indicating these materials' ability to absorb water from the surrounding environment[43].

In addition, the broadband spectrum of clay indicates the potential for water hydration in the adsorbent at 3436 and 1635 cm^{-1} in sample P1, and at 1638 cm^{-1} in sample P2. Moreover, the presence of feldspar is indicated by splitting bands in the 800-400 cm 1 region, including 778, 692, and 458 cm^{-1} and one band at 1041 cm^{-1} in samples P1 and P2. The absorption bands at 3435, 1045, 914, 778, 692, and 458 cm 1 indicated the presence of kaolinite in all samples[44].

Unedited version published online on 18/10/2023

Furthermore, the fired-clay (meta-clay) is visible between 1032 and 1094 cm. Furthermore, quartz was found in sample P1 at 778, 692, and 458 cm^{-1} and in sample P2 at 778, 692, and 458 cm^{-1}. Besides, calcite was found in samples P1 and P2 at 1383 and 692 cm^{-1}, respectively. Moreover, the potsherds were in contact with soil containing a high percentage of salt. Na, Cl, and Ca concentrations are greater in the red area than in the black incompletely fired parts[45].

Unedited version published online on 18/10/2023

Conclusions

This study concerns the phenomenon of salt fog on the surface of potsherds from the Saqqara excavation. Saqqara has had great historical value and cultural importance for thousands of years. Salts are strongly related to temperature, humidity, rainfall, wind, air pressure, etc. The microscopic investigation showed a thick distribution of salt on the potsherd surface and an overlap among the salt and sand layers scattered on the surface. Cubic crystals formed in the middle of low-concentration droplets. Furthermore, the salts sediment over the body's surface when the evaporation rate exceeds the solution's supply rate and the dried cubic salts appear clearly on it. The findings indicate that the interfacial characteristics influence where and how crystals form. SEM-EDX results of the samples showed a high ratio of chloride salts content reaching 53.42% in sample P1 and 32.8% in sample P2. In addition, sulfate salts are a minor proportion in the sample P1 of 0.29%. Regarding XRD analysis, results show that both pottery samples contain salts, especially sodium chloride, but the percentage of salts in the first sample is much higher than that of the second sample. In addition, XRD and FTIR analysis confirmed the results of SEM-EDX in the presence of a large percentage of halite salt. These results helped us make a good diagnosis of the crystallized salts on the archaeological potsherds. These findings will determine the most effective ways of extracting salts from archaeological pottery.

Acknowledgements

The authors would like to thank Prof. Dr. Ola El-Augizi, who is in charge of the Faculty of Archeology's excavations at the Saqqara site, for her assistance and encouragement during the research. The writers further acknowledge Prof. Dr. Tariq Tawfiq, Dr. Nader Elhosiny, Mr. Magdi Al-Beheiri, Mr. Montasir Kamal, and Mrs. Weaam Ashour for their earnest efforts.

Conflicts of interest: authors declare that they have no conflict of interest.

APPENDIX

List of symbols

q= quantity of water vapor (g)

Q=quantity of heat (cal)

dp/dR' = vapor-density gradient (g/cm^3)

dT/dR' = temperature gradient (K/cm)

R'= radial distance (cm)

D= diffusion coefficient of water vapor in air (cm^2/sec)

k= heat-conduction coefficient of moist air ($cal\ cm^{-1}\ sec^{-1}\ deg^{-1}$)

c_p= specific heat of water at constant pressure ($cal\ g^{-1}\ deg^{-1}$)

T=temperature of droplet (deg)

r= radius of droplet (cm)

t= time (seconds)

m= mass of droplet (g)

Unedited version published online on 18/10/2023

References

1. Sáenz-Martínez, A., Pérez-Estébanez, M., Andrés, M. S., de Buergo M. A., and Fort, R., Efficacy of acid treatments used in archaeological ceramics for the removal of calcareous deposits. *Eur. Phys. J. Plus.*, 2021, **136**, 1–16.
2. Khalifa, E., and Abd Elrahim, E., Identification of vessel use and explanation of change in production techniques from the Old to the Middle Kingdom: Organic residue analysis, fabric and thermal characterization of pot sherds from Qubbet el-Hawa, Aswan, Egypt. *Archaeometry*., 2020, **62**(6), 1115–1129.
3. Ibrahim, M. M., and Mohamed, H. M., Analytical Study and Conservation of New Kingdom Period Pottery Jars from Saqqara Excavation, Egypt. *Adv. Mater. Res.*, 2021, **1167**, 101–113.
4. Wodzińska, A., A Manual of Egyptian Pottery. **Volume 3**, Second Intermediate Period–Late Period, Ancient Egypt Research Associates, Inc. Boston, 2010.
5. Mohamed, H. M., and Mohamed, W. S., Evaluating nano Primal AC33 for protection and consolidation processes of archaeological pottery: a comparison study with silica and montmorillonite nanoparticles. *Pigment. Resin. Technol*. 2023, https://doi.org/10.1108/prt-09-2022-0104.
6. Ibrahim, M. M., Mohamed, W. S., and Mohamed, H. M., Evaluation of the Efficacy of Traditional and Nano Paraloid B72 for Pottery Consolidation. *Int. J. Conserv. Sci.*, 2022, **13**, 15–30.
7. Sena da Fonseca, B. S., Simao, J. A. R., and Galhano, C., Effect of Coastal Environment in Clay Facing Bricks and Roof Tiles. 1st Annual International Interdisciplinary Conference, AIIC, Azores, Portugal, 2013.

Unedited version published online on 18/10/2023

8. Ibrahim, M. M., Mohamed, W. S., and Mohamed, H. M., Experimental study for evaluation of Paraloid® B72 and its nanocomposite with nano TiO_2 and nano ZnO for consolidation of pottery samples. *Sci. Cult.*, 2021, **7**, 101–111.
9. Lubelli, B., Hees, R. P. J., and Groot, C. J. W. P., Sodium chloride crystallization in a "salt transporting" restoration plaster. *Cem. Concr. Res.*, 2006, **36**, 1467–1474.
10. Angeli, M., Hébert, R., Menéndez, B., David, C., and Bigas, J. P., Influence of temperature and salt concentration on the salt weathering of a sedimentary stone with sodium sulphate. *Eng. Geol.*, 2010, **115**, 193–199.
11. Di Benedetto, C., Cappelletti, P., and Favaro, M., Porosity as key factor in the durability of two historical building stones: Neapolitan Yellow Tuff and Vicenza Stone. *Eng. Geol.*, 2015, **193**, 310–319.
12. Angeli, M., Benavente, D., Bigas, J. P., Menendez, B., Hebert, R., and David, C., Modification of the porous network by salt crystallization in experimentally weathered sedimentary stones. *Mater Struct.*, 2008, **41**, 1091–1108.
13. Benavente, D., Garcia del Cura, M. A., Garcia-Guinea, J., Sanchez-Moral, S., and Ordonez, S., Role of pore structure in salt crystallisation in unsaturated porous stone. *J. Cryst. Growth.*, 2004, **260**, 532–544.
14. Zornoza-Indart, A., López-Arce, P., Simão, J., Leal, N., and Zoghlami, K., Accelerated aging experiments with saline fog, involving ventilation in calcarenitic monument rocks. *Comun. Geol.*, 2014, **101**, 1181–1185.
15. Scrivano, S., and Gaggero, L., An experimental investigation into the salt-weathering susceptibility of building limestones. *Rock. Mech. Rock. Eng.*, 2020, **53**, 5329–5343.

Unedited version published online on 18/10/2023

16. Ottosen, L. M., Pedersen, A. J., and Rorig-Dalgaard, I., Salt-related problems in brick masonry and electrokinetic removal of salts. *J. Build. Apprais.*, 2007, **3**(3), 181–194.
17. Silva, Z. S. G. S., and Imão, J. A. R., The role of salt fog on alteration of dimension stone. *Constr. Build. Mater.*, 2009, **23**, 3321–3327.
18. Quilaqueo, M., and Aguilera, J. M., Crystallization of NaCl by fast evaporation of water in droplets of NaCl solutions. *Int. Food Res. J.*, 2016, **84**, 143–149.
19. Cardell, C., Delalieux, F., Roumpopoulos, K., Moropoulou, A., Auger, F., and Van Grieken, R., Salt-induced decay in calcareous stone monuments and buildings in a marine environment in SW France. *Constr Build Mater.*, 2003, **17**, 165–179.
20. Bracciale, M. P., Sammut, S., Cassar, J., Santarelli, M. L., and Marrocchi, A., Molecular Crystallization Inhibitors for Salt Damage Control in Porous Materials: *An Overview. Molecules.*, 2020, **25**, 1873.
21. Mohamed, H. M., Study and characterization of Old Kingdom period potsherds from Abusir excavation. A case study. *J. Sci. Arts.*, 2022, **22**(3), 723–734.
22. Naillon, A., Duru, P., Marcoux, M., and Prat, M., Evaporation with sodium chloride crystallization in a capillary tube. *J. Cryst. Growth.*, 2015, **422**, 52–61.
23. Çelik, M. Y., and Aygün, A., The effect of salt crystallization on degradation of volcanic building stones by sodium sulfates and sodium chlorides. *Bull. Eng. Geol. Environ.*, 2019, **78**, 3509–3529.
24. Vázquez, P., Thomachot-Schneider, C., Mouhoubi, K, Fronteau G., Gommeaux, M., Benavente, D., Barbin, V., and Bodnar, J. L., Infrared Thermography monitoring of the NaCl crystallisation process. *Infrared. Phys. Technol.*, 2015, **71**, 198–207.
25. Shahidzadeh-Bonn, N., Rafai, S., Bonn, D., and Wegdam,, G., Salt Crystallization during Evaporation. *Langmuir*, 2008, **24**, 8599–8605.

Unedited version published online on 18/10/2023

26. Feliciano, I., Cerâmica Arqueológica: estudo comparativo da eficácia de consolidantes aplicados no processo de dessalinização, Dissertação para obtenção do grau de Mestre em Conservação e Restauro, Faculdade de Ciências e Tecnologia (FCT) FCT Departamentos FCT: Departamento de Conservação e Restauro FCT: DCR, Universidade de Lisboa, Portugal, 2016.
27. Broström, M., Enestam, S., Backman, R., Mäkelä, K., Condensation in the KCl–NaCl system. *Fuel Process. Technol.* 2013, **105,** 142–148.
28. Keith, C. H., Arons, A. B., The Growth of Sea Salt Particles by Condensation Of Atmospheric Water Vapor. *J. Atmos. Sci.,* 1954, **11,** 173-184.
29. Yarom, M., Marmur, A. Capillary condensation with a grain of salt. *Langmuir*, 2017, **106,** 13444-13450.
30. Mohamed, H. M., A Comparison Study of Titanium Dioxide and Zinc Oxide Nanoparticles for Cleaning Archaeological Pottery. *J. Nano Res.*, 2022, **76**, 61–77.
31. Tite, M. S., Pottery Production, Distribution, and Consumption-The Contribution of the Physical Sciences. *J. Archaeol. Method. Theory.*, 1999, **6**(3), 181–233.
32. Grammatikakis, I. E., Kyriakidis, E., Demadis, K. D., Diaz, A. C., and Leon-Reina, L., Mineralogical Characterization and Firing Temperature Delineation on Minoan Pottery, Focusing on the Application of Micro-Raman Spectroscopy. *Heritage.*, 2019, **2**, 2652–2664.
33. Olivares, M., Zuluaga, M. C., Ortega, L. A., Murelaga, X., Alonso-Olazabal, A., Urteaga, M., Amundaray, L., Alonso-Martin, I., and Etxebarriaa, N., Characterisation of fine wall and eggshell Roman pottery by Raman spectroscopy. *J. Raman. Spectrosc.*, 2010, **41**, 1253–1259.
34. Kiliç, N. Ç., Kiliç, S., and Akgül, H. Ç., An archaeometric study of provenance and firing technology of halaf pottery from tilkitepe (Eastern Turkey). *Mediterr. Archaeol. Archaeom.*, 2017, **17**(2), 35–48.

Unedited version published online on 18/10/2023

35. Poppe, L. J., Paskevich, V. F., Hathaway, J. C., and Blackwood, D. S., A Laboratory Manual for X-Ray Powder Diffraction. U.S. Geological Survey Open-File Report 01-041, 2001.
36. Abd Elrahim, E., and Weshahy, I., The mortar damage and its harmful effects on the glazed ceramic tiles in Terbana Mosque-Alexandria, Egypt. *Shedet.*, 2017, **4**, 155–166.
37. Abd-Allah, R., Al-Muheisen, Z., and Al-Howadi, S., Cleaning strategies of pottery objects excavated from Khirbet Edh-Dharih and Hayyan Al-Mushref, Jordan: four case studies. *Mediterr. Archaeol. Archaeom.*, 2010, **10**(2), 97–110.
38. De Nolf, W., Dik, J., Vandersnickt, G., Wallertc, A., and Janssensa, K., High-energy X-ray powder diffraction for the imaging of (hidden) paintings. *J. Anal. At. Spectrom.*, 2011, **26**, 910–916.
39. Veld, B., and Durc, I. C., Archaeological Ceramic materials Origin and Utilization, Utilization (Natural Science in Archaeology)- Softcover reprint of the original 1st ed., 1999.
40. Al-Naddaf, M., Provenance and firing technology of Iron Age pottery of Tell Johfiyeh, Northern Jordan, Yarmouk University, 2006, **22**(4),149–165.
41. Madejova, J., FTIR techniques in clay mineral studies. *Vib. Spectrosc.*, 2003, **31**, 1–10.
42. Drob, A., Vasilache, V., and Bolohan, N., The Interdisciplinary Approach of some Middle Bronze Age Pottery from Eastern Romania. *Appl. Sci.*, 2021, **11**, 4885.
43. Nayak, P. S., and Singh, B. K., Instrumental characterization of clay by XRF, XRD and FTIR. *Bull. Mater. Sci.*, 2007, **30**, 235–238.
44. Jozanikohan, G., and Abarghooei, M. N., The Fourier transform infrared spectroscopy (FTIR) analysis for the clay mineralogy studies in a clastic reservoir. *J. Pet. Explor. Prod. Technol.*, 2022, **12**, 2093–2106.

Unedited version published online on 18/10/2023

45. Vasilache, V., Kavruk, V., and Tencariu, F., OM, SEM–EDX, and micro-FTIR analysis of the Bronze Age pottery from the Baile Figa salt production site (Transylvania, Romania). *Microsc. Res. Tech.*, 2020, **83**, 604–617.

Unedited version published online on 18/10/2023

Table 1. Demonstrates the potsherds' description.

Code sample	Potsherds' Description
P1	It is a reddish-brown potsherd that is 1.1 cm thick and measures 22.4 cm long by 8.8 cm wide. It suffers from heavy crystallization of salts on the surface
P2	It is a dark brown potsherd that is 1.4 cm thick and measures 9.6 cm long by 7.3 cm wide. It has a dry layer of salt droplets on the surface of the potsherd.

Unedited version published online on 18/10/2023

Table 2. Reveals the potsherd samples' elemental concentration (Wt. %) by SEM-EDX.

Sample code	Elements									
	O	Na	Mg	Al	Si	S	Cl	K	Ca	Fe
P1	8.39	30.31	0.43	0.82	1.71	0.29	53.42	0.45	2.55	1.63
P2	19.18	22.98	0.8	3.74	8.63	--	32.8	1.4	2.9	7.57

Unedited version published online on 18/10/2023

Table 3. X-Ray diffraction results for potsherd components (%).

Sample code	Component						
	Quartz	Diopside	Albite	Halite	Hematite	Muscovite	Magnetite
P1	50	12.4	--	28.9	5.3	--	3.4
P2	35.6	11	24.2	18.9	--	10.3	--

Unedited version published online on 18/10/2023

Table 4. FTIR results for potsherd components (cm^{-1})

Sample code	Wavenumber cm^{-1}										
	1	2	3	4	5	6	7	8	9	10	11
P1	3841	3756	3436	2919	2851	1635	1383	1041	778	692	458
P2	3435	2918	2850	1638	1383	1045	778	692	458	--	--

Unedited version published online on 18/10/2023

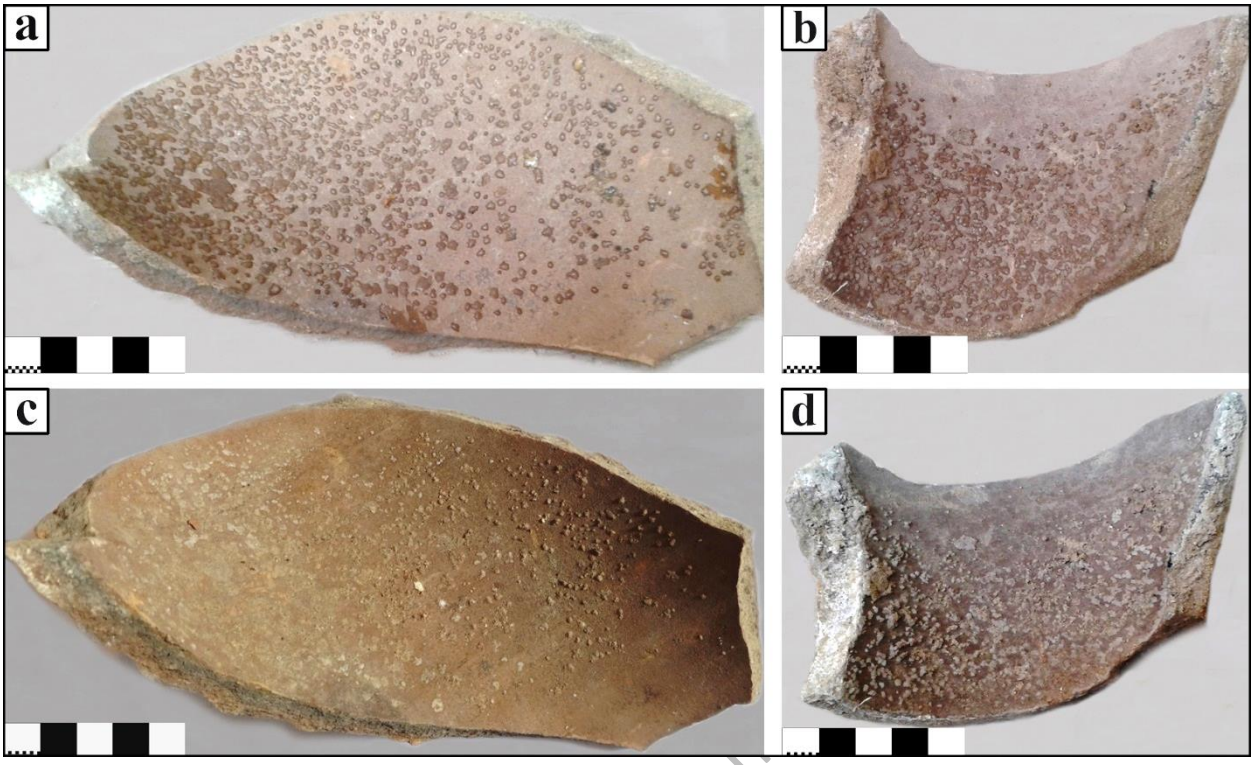

Figure 1. Shows the potsherds before and after drying of saline solution.
(a, c) sample P1, and (b, d) sample P2.

Unedited version published on

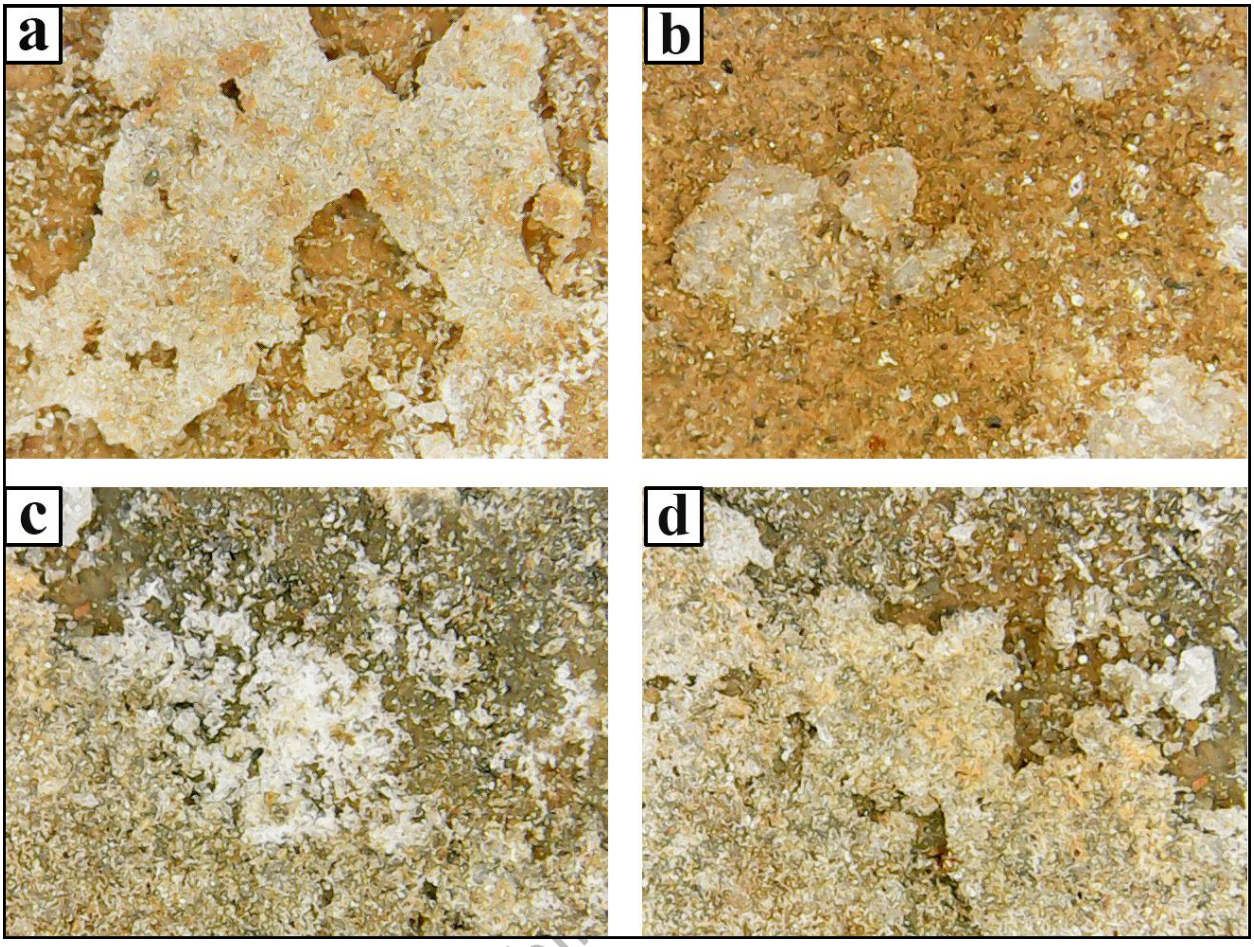

Figure 2. Shows the salt crystallization on the potsherds. (a, b) sample P1, and (c, d) sample P2.

Unedited version pub

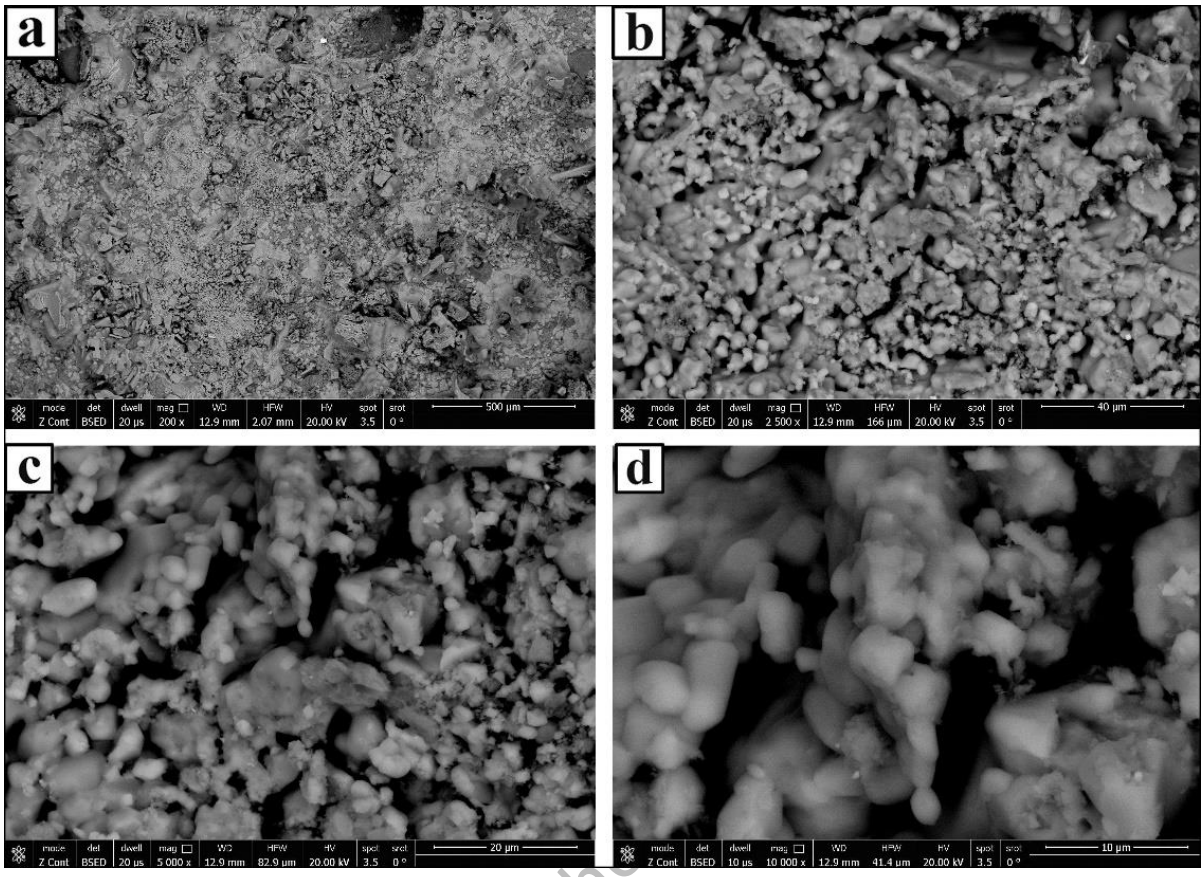

Figure 3. Demonstrates the findings of the SEM investigation of sample P1.

Unedited version published

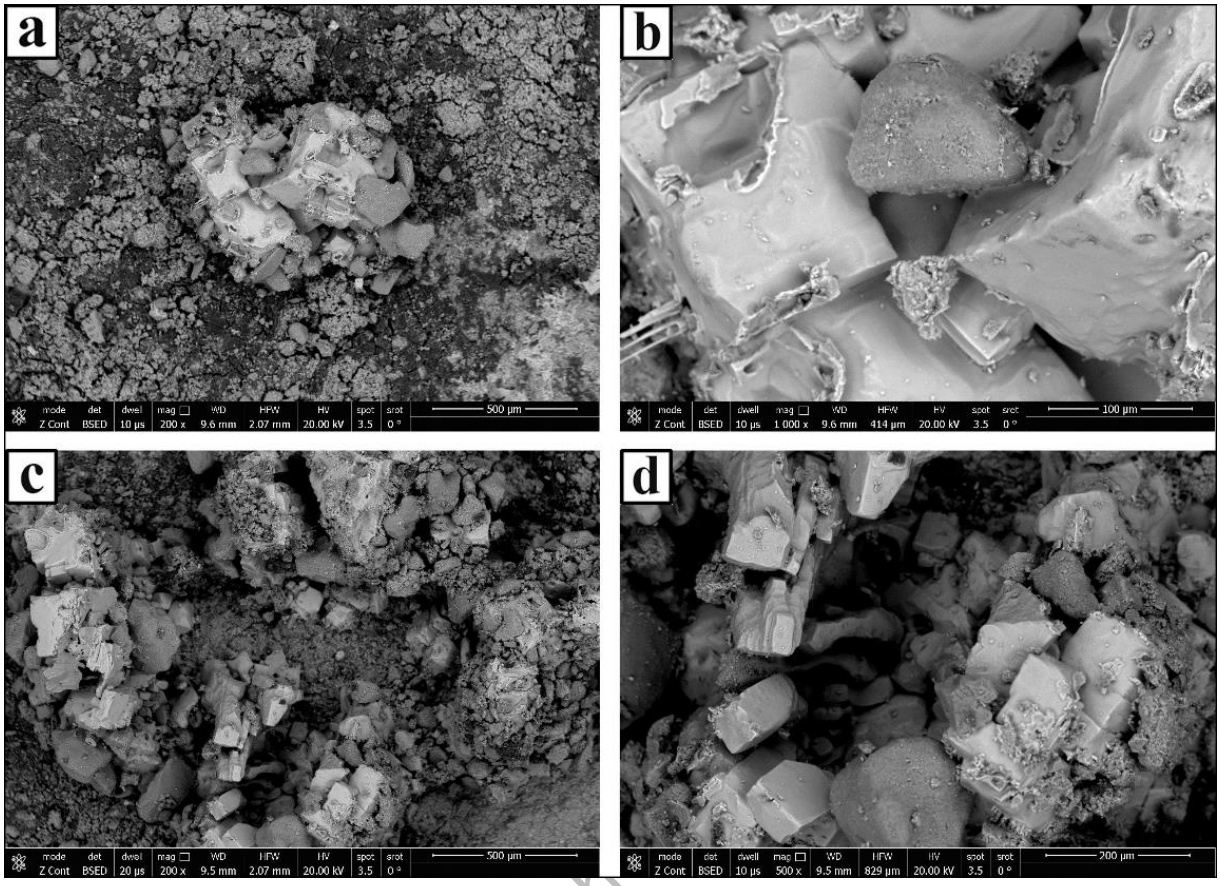

Figure 4. Shows the results of the SEM investigation of sample P2.

Unedited version published

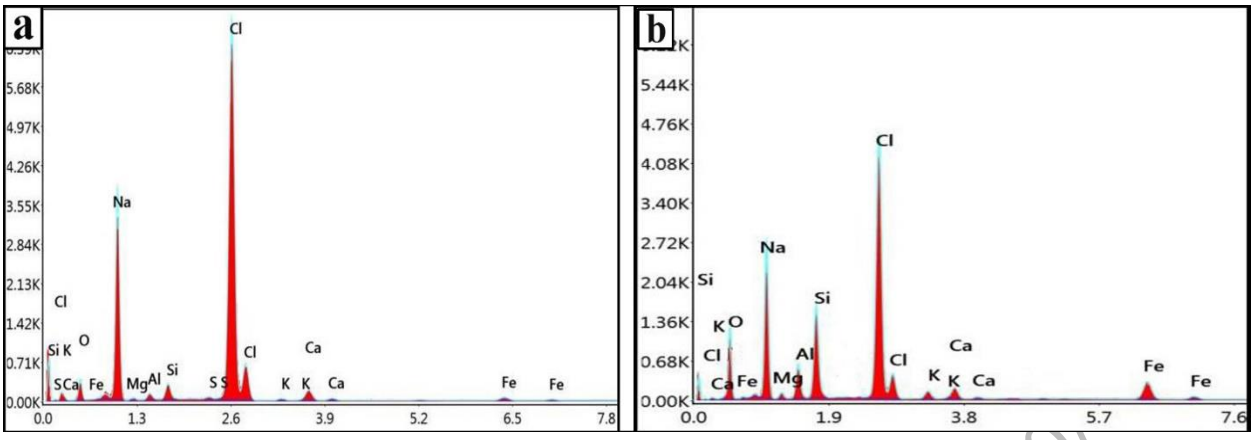

Figure 5. Displays the SEM - EDX results. (a) Sample P1, and (b) sample P2.

Unedited version published online on 18/10/

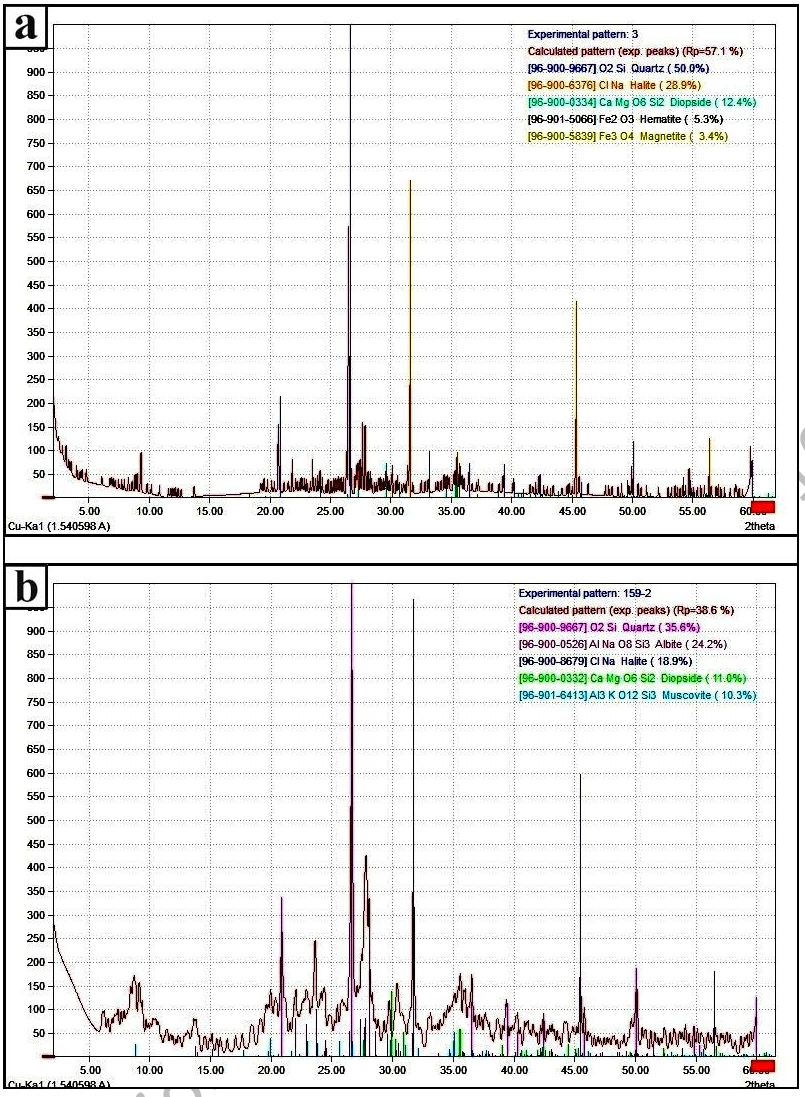

Figure 6. XRD patterns of the potsherds samples. (a) Sample P1, and (b) sample P2.

Unedited version

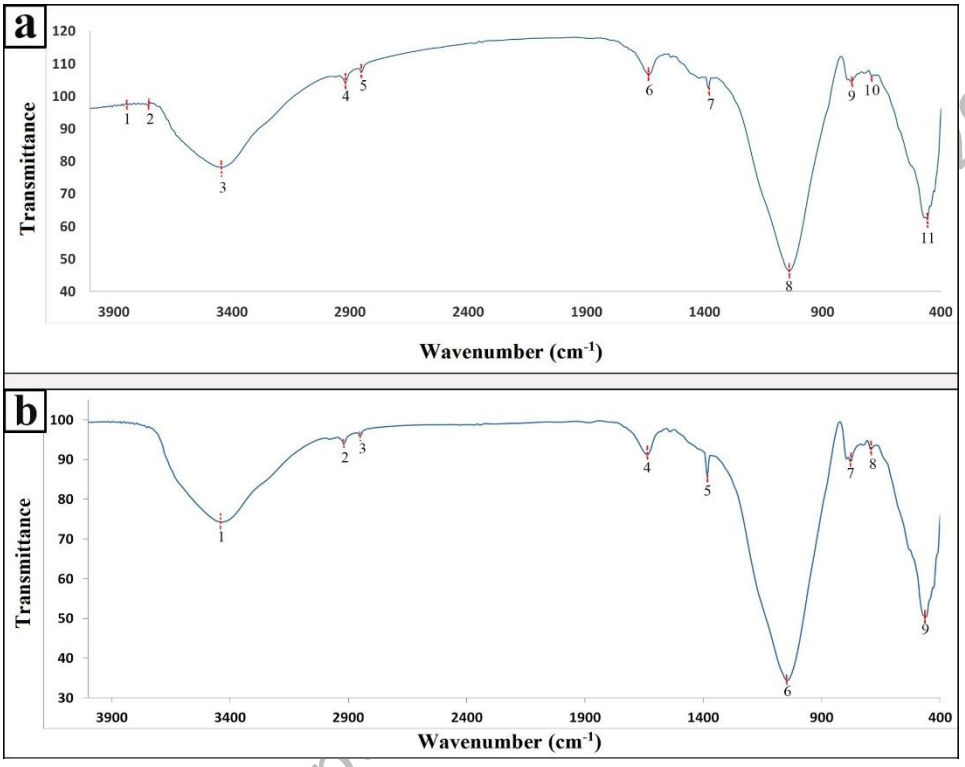

Figure 7. FTIR bands of the potsherds samples. (a) Sample P1, and (b) sample P2.

Unedited version p 2023